International Astronomy and Astrophysics Research Journal

Volume 8, Issue 1, Page 116-124, 2026; Article no.IAARJ.166147

Statistical Associations among C-Class Solar Flares, Ionospheric TEC, Plasma Temperatures, and Solar-Activity Indices (January-March 2025)

Ashish Kumar Meena [a++*]

[a] *Department of Physics, SR University, Warangal, Telangana, India.*

Author's contribution

The sole author designed, analyzed, interpreted and prepared the manuscript.

Article Information

DOI: https://doi.org/10.9734/iaarj/2026/v8i1129

Open Peer Review History:
This journal follows the Advanced Open Peer Review policy. Identity of the Reviewers, Editor(s) and additional Reviewers, peer review comments, different versions of the manuscript, comments of the editors, etc are available here: https://pr.sdiarticle5.com/review-history/166147

Original Research Article

Received: 03/07/2026
Accepted: 10/09/2026
Published: 19/09/2026

Abstract

Aims: To characterise the distributions and pairwise associations among C-class solar-flare magnitude, duration, ion temperature (Ti), electron temperature (Te), total electron content (TEC), solar zenith angle (SZA), sunspot number (SSN), and 10.7 cm solar radio flux (F10.7) in an author-compiled January-March 2025 dataset, while distinguishing descriptive covariance from event-centred ionospheric flare responses.
Study Design: Exploratory descriptive observational analysis of co-tabulated solar and ionospheric variables.
Place and Duration of Study: Public space-weather records compiled for 1 January to 18 March 2025, a 77-calendar-day interval; 75 days are represented in the retained source compilation.
Methodology: The dataset contains 624 C-class flares. Flare magnitude and duration were summarised together with Ti, Te, absolute TEC, SZA, SSN, and F10.7. Pearson coefficients were used descriptively. Correlations involving TEC used 623 records because one TEC entry was missing; analyses not involving

[++] *Postdoctoral Fellow;*
**Corresponding author: E-mail: ashishmeena944@gmail.com;*

Cite as: *Meena, A. K. (2026). Statistical Associations among C-Class Solar Flares, Ionospheric TEC, Plasma Temperatures, and Solar-Activity Indices (January-March 2025). International Astronomy and Astrophysics Research Journal, 8(1), 116–124. https://doi.org/10.9734/iaarj/2026/v8i1129*

TEC used 624 records. Repeated same-day solar-index values mean that event-level coefficients are flare-record-weighted rather than day-independent estimates. Product-level metadata on station, altitude, geographical coordinates, and retrieval for TEC/Ti/Te, as well as the terrestrial reference location used for SZA, were not retained; therefore, no causal or p-value-based inference is made.
Results: Mean flare magnitude was C3.87 and mean duration was 19.9 min. Flare magnitude showed its largest positive descriptive association with F10.7 (r = 0.331), followed by SZA (r = 0.227) and SSN (r = 0.146), whereas its association with absolute TEC was negligible (r = 0.032). Mean Ti and Te were 1168 K and 1694 K, respectively, with a mean Ti/Te ratio of approximately 0.70.
Conclusion: The results characterise association patterns within the retained dataset during an active interval of Solar Cycle 25. The near-zero magnitude-TEC correlation concerns absolute TEC and does not establish an absence of C-class flare effects. Event-centred analysis requires traceable high-cadence ionospheric measurements, explicit spatial and geomagnetic controls, and recoverable product provenance.

Keywords: C-class solar flares; total electron content; ion temperature; electron temperature; F10.7; solar zenith angle; ionosphere; space weather.

1. Introduction

Solar flares produce rapid enhancements in soft X-ray and extreme-ultraviolet (EUV) irradiance that increase ionisation in the sunlit terrestrial atmosphere, often in association with coronal mass ejections (Meena *et al*., 2022) and, at higher particle energies, ground-level cosmic-ray enhancements (Gopalswamy *et al*., 2012). GNSS-derived total electron content (TEC) and its time derivative are therefore widely used to examine flare-associated ionospheric disturbances (Liu *et al*., 2006), including during major geoeffective events such as the September 2017 storms (Meena & Gour, 2024; Zhang *et al*., 2019). The magnitude of the ionospheric response is not determined by GOES soft X-ray class alone. Event geometry, the EUV spectral enhancement, solar zenith angle, latitude, local time, season, and the pre-existing ionospheric state can all influence the measured response (Le *et al*., 2013; Zhang *et al*., 2011).

C-class flares, defined by a GOES 0.1-0.8 nm peak soft X-ray flux from 10^{-6} to less than 10^{-5} W m^{-2}, are much more frequent than M- and X-class events. Their ionospheric signatures are correspondingly more difficult to isolate from background variability. A recent low-latitude analysis of 396 C-class flares during the peak of Solar Cycle 24 found that differential vertical TEC responses to C-class events were weak and strongly dependent on the method used to estimate the flare-associated perturbation (Saharan *et al*., 2023). This makes large-sample descriptive studies useful, provided that correlations involving absolute TEC are not interpreted as direct measurements of flare-induced ΔTEC.

Background solar and geomagnetic variability is also important. TEC responds to solar forcing on multiple timescales; it may covary with geomagnetic indices, solar ultraviolet and X-ray irradiance, and F10.7, sometimes with temporal lags, and can vary seasonally or during periods affected by geomagnetic storms and solar flares (Feng *et al*., 2023; Morozova *et al*., 2020; Tsugawa *et al*., 2006; Vaswani *et al*., 2022). Plasma temperatures likewise depend on altitude, latitude, local time, season, and solar activity; global empirical studies show that Te and Ti cannot be interpreted reliably without these contextual coordinates (Köhnlein, 1986; Truhlik *et al*., 2009).

However, the retained January–March 2025 compilation has not yet been characterised through a joint descriptive assessment of flare magnitude, duration, plasma temperatures, TEC, SZA, SSN, and F10.7 that explicitly distinguishes dataset-level covariance from event-centred flare response.

The present study therefore adopts an explicitly exploratory objective. It characterises the distributions and pairwise associations among C-class flare magnitude, duration, Ti, Te, TEC, SZA, SSN, and F10.7 in the author-compiled January-March 2025 dataset. The objectives are to (1) summarise the statistical distribution of the flare population; (2) describe association patterns among the tabulated solar and ionospheric variables; and (3) identify which interpretations are supported by the available data and which require event-centred, spatially resolved analysis.

2. Methodology

2.1 Data Sources and Scope

The dataset comprises 624 C-class solar flares compiled for the interval 1 January to 18 March 2025. The retained source compilation identifies public space-weather records from NOAA/SWPC, the Solar Influences Data Analysis Center (SIDC), and NASA as the basis of the event table, but it does not preserve variable-level product identifiers, archive paths, product versions, or retrieval dates. For each event, the compiled fields include flare classification (for example, C5.1), start, maximum, and end times in UT, Ti (K), Te (K), TEC (TECU, where 1 TECU = 10^{16} electrons m^{-2}), SZA (degrees), SSN, and F10.7 (solar flux units, sfu). One initial TEC entry was marked missing and was excluded from analyses involving TEC.

Product-level station, altitude, geographic-coordinate, measurement/model status, cadence, and retrieval identifiers for TEC, Ti, and Te were not retained in the compiled event table. The terrestrial reference location and precise timestamp convention used for the co-tabulated SZA values were likewise not retained. These variables are therefore treated here as contextual parameters from the retained compilation rather than as independently reconstructable, site-resolved measurements. This constraint permits description of associations within the compiled dataset but precludes causal attribution of changes in TEC or plasma temperature to individual flares and precludes a unique physical interpretation of SZA-dependent correlations.

The calendar interval contains 77 days. The retained source compilation reports records on 75 represented days within that interval. The retained metadata do not establish whether the two unrepresented calendar dates correspond to zero C-class events or to unretained/missing source records. To avoid implying documented observational coverage, flare occurrence is therefore reported both per represented day in the source compilation (624/75 = 8.32) and per calendar day across the complete interval (624/77 = 8.10).

2.2 Derived Parameters

Flare magnitude was represented by the numerical coefficient following the letter C (range 1.0-9.9). Flare duration was calculated as the end time minus the start time, with day-boundary crossings accommodated, and expressed in minutes. The Ti/Te ratio was calculated for each event for which both temperatures were present. Daily counts and daily means of TEC, F10.7, SSN, and flare magnitude were also derived for graphical summary. SZA was analysed as supplied in the retained compilation; because its terrestrial reference location and timestamp convention are unavailable, no new geometric derivation or site-specific interpretation of SZA was attempted. The retained study materials do not provide a sufficiently detailed extraction log to reconstruct duplicate-report handling, overlapping-event resolution, or all variable-matching rules, and no such details are inferred here.

2.3 Statistical Analysis

Descriptive statistics included the mean, median, range, standard deviation, and quartiles where available in the compiled analysis. Pearson product-moment correlation coefficients were calculated among flare magnitude, duration, Ti, Te, TEC, SZA, SSN, and F10.7. Correlations involving TEC used $n = 623$ records because one TEC entry was missing; correlations not involving TEC used $n = 624$ records. The coefficients are interpreted descriptively rather than as independent inferential tests. F10.7 and SSN may take repeated same-day values for multiple flares, so days with more flare records contribute those daily values more often and the resulting event-level coefficients are flare-record-weighted rather than equal-day-weighted estimates. Ordinary Pearson correlation relies on independence for inferential interpretation, and repeated or clustered observations can otherwise produce misleading inference (Bakdash & Marusich, 2017). Accordingly, no p-value-based claims of statistical significance are made from the event-level correlation matrix, and no cluster-adjusted inferential model is claimed.

Visualisations include the flare-magnitude distribution, daily event counts, TEC versus flare magnitude, temperature distributions by magnitude bin, a Pearson correlation heatmap, daily mean TEC and F10.7, flare duration versus magnitude, and the Ti/Te distribution. Regression lines shown in the figures are descriptive visual aids only. Because the dataset contains absolute TEC rather than a documented pre-flare/post-flare perturbation series, the magnitude-TEC coefficient is not used as a direct flare-response estimator. Event-centred approaches based on ΔTEC or TEC rate-of-change are more appropriate for causal flare-response analysis (Liu *et al*., 2006; Saharan *et al*., 2023). The absence of a day-clustered or equal-day-weighted sensitivity analysis is treated as a limitation when interpreting coefficients that contain repeated daily indices.

3. Results

3.1 Overall Characteristics of the Flare Population

A total of 624 C-class flares were represented in the compiled dataset. The mean occurrence was 8.32 flares per represented day in the source compilation and 8.10 flares per calendar day over the 77-day study interval. Because the retained metadata do not distinguish zero-event from missing/unretained status for the two calendar dates not represented, the calendar-day rate is the more transparent full-interval denominator. The maximum daily count was 21 events on 12 March 2025. The magnitude distribution was concentrated toward weaker C-class events: the mean magnitude was C3.87 and the median was C3.35, with C2-C4 events comprising the largest part of the distribution. Fourteen events exceeded C9.0.

Mean flare duration was 19.9 min and the median was 16 min. The distribution was right-skewed, with most events clustered at shorter durations and a smaller number of longer-duration events (Figs. 1a and 3a). Ti ranged from 980 to 1506 K with a mean of 1168 K, whereas Te ranged from 1319 to 2260 K with a mean of 1694 K. The mean Ti/Te ratio was approximately 0.70. TEC ranged from 4.3 to 32.1 TECU, with a mean of 13.6 TECU.

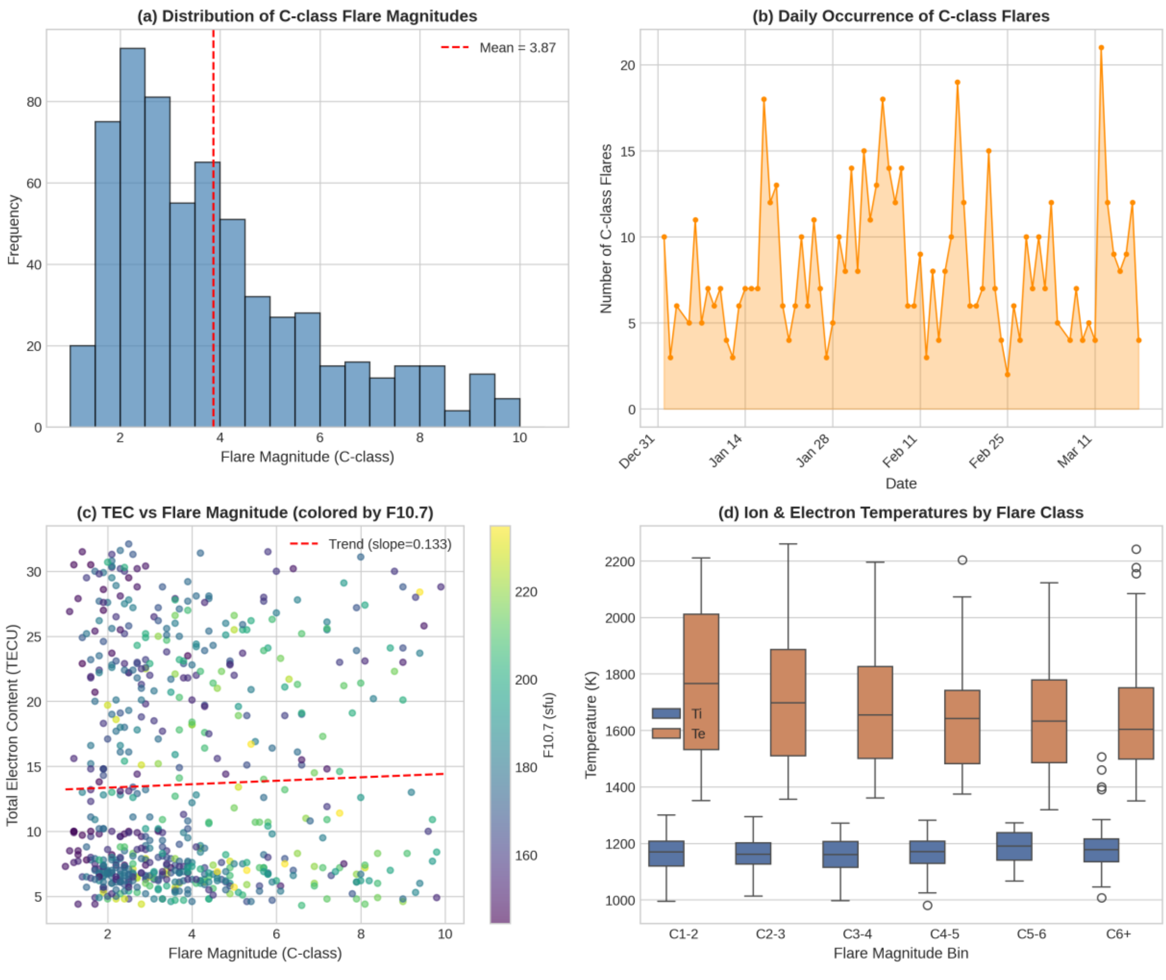

Fig. 1. Overview of the 624-event C-class flare dataset (1 January-18 March 2025): (a) flare-magnitude distribution; (b) daily occurrence counts; (c) absolute TEC versus flare magnitude, colored by F10.7; and (d) Ti and Te distributions by flare-magnitude bin. The regression line in panel (c) is descriptive and does not represent an event-centred flare-response estimate

3.2 Correlation Structure

The Pearson matrix (Fig. 2a) shows that flare magnitude had its largest positive descriptive coefficient with F10.7 (r = 0.331; n = 624), a weak-to-moderate association, followed by SZA (r = 0.227; n = 624) and SSN (r = 0.146; n = 624). The association between flare magnitude and absolute TEC was negligible (r = 0.032; n = 623). Electron temperature was negatively associated with SZA (r = -0.573; n = 624) and more weakly with flare magnitude (r = -0.185; n = 624). Ti was positively associated with Te (r = 0.372; n = 624) and F10.7 (r = 0.276; n = 624). These coefficients are descriptive and should not be interpreted as day-independent estimates when daily indices are repeated across multiple flare records.

These coefficients describe the covariance structure of the compiled variables; they do not by themselves establish flare-driven physical changes. In particular, the near-zero magnitude-TEC coefficient does not test whether TEC increased immediately after individual C-class flares because no documented pre-flare baseline or event-centred ΔTEC variable was used.

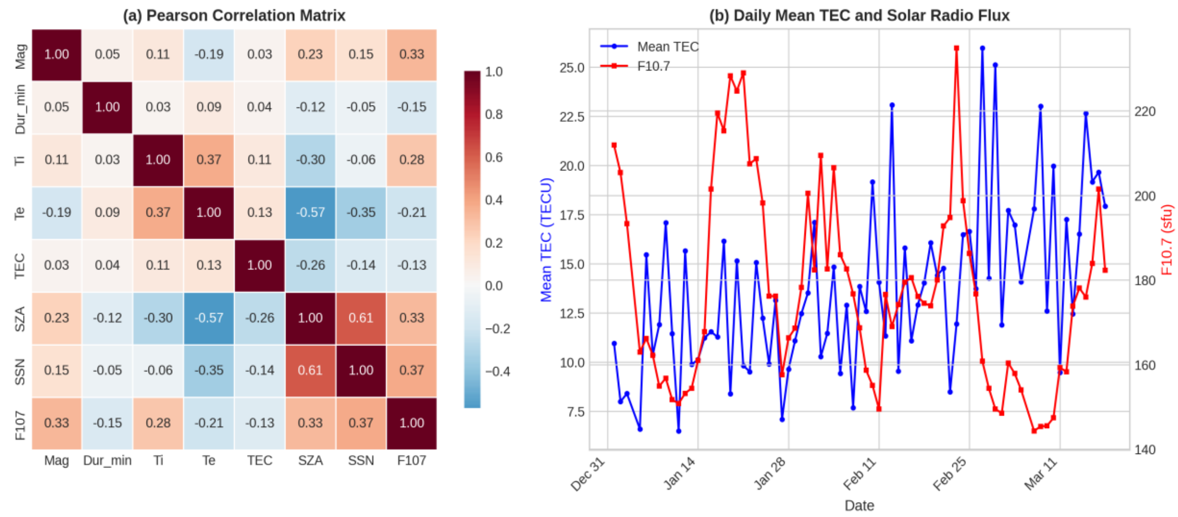

Fig. 2. (a) Pearson correlation matrix for the principal variables in the compiled 624-event dataset; (b) daily mean absolute TEC and concurrent F10.7. Event-level coefficients involving repeated daily indices are descriptive, flare-record-weighted summaries rather than independent day-level estimates

3.3 Temporal Evolution and Duration Characteristics

Daily mean TEC and F10.7 varied substantially throughout the study interval and did not show consistent day-to-day co-movement (Fig. 2b). Flare duration was nearly independent of flare magnitude in the Pearson analysis (r = 0.052) and showed a weak negative association with F10.7 (r = -0.150). The Ti/Te distribution was centred close to 0.70, with most observations between approximately 0.55 and 0.85 (Fig. 3b).

4. Discussion

4.1 Interpreting the Weak Magnitude-TEC Association

The most important interpretative point is that r = 0.032 concerns flare magnitude versus absolute TEC, not flare magnitude versus flare-induced ΔTEC. Absolute TEC contains substantial background variability related to illumination geometry, local time, season, solar activity, geomagnetic forcing, transport, and the pre-existing ionospheric state. Studies designed specifically to quantify flare effects therefore use high-cadence differential TEC, rate-of-TEC change, quiet-day baselines, or other event-centred approaches (Liu *et al*., 2006; Zhang *et al*., 2019), including comparisons of strong- and weak-flare TEC responses at a single solar-cycle peak (Meena *et al*., 2024).

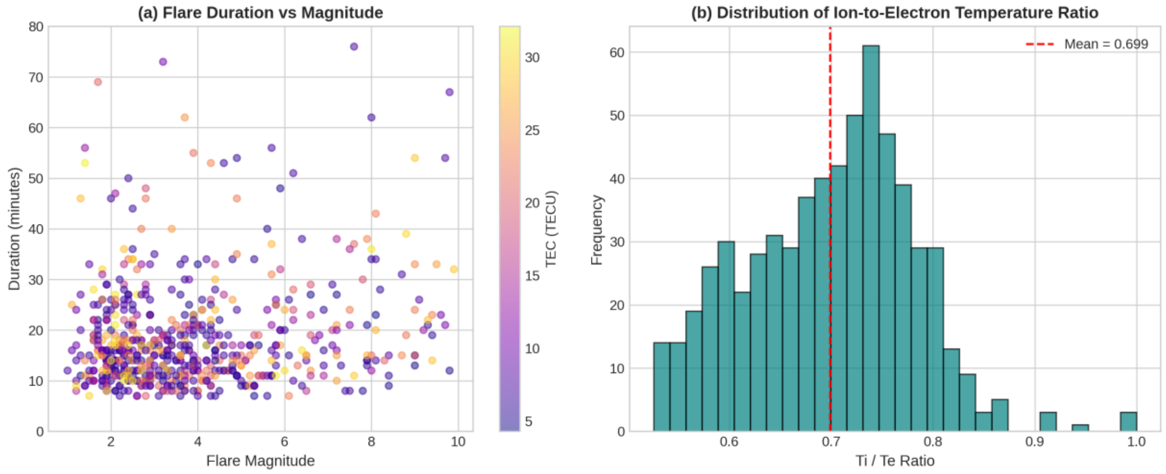

Fig. 3. (a) Flare duration versus magnitude, colored by absolute TEC; (b) distribution of the Ti/Te ratio. These plots summarize the compiled data and are not intended as causal flare-response diagnostics

The present weak association is nevertheless compatible with the broader observation that lower-class flares often have small and heterogeneous TEC signatures. Saharan *et al.* (2023), using GPS-derived differential VTEC for 396 C-class flares during 2014 at low latitude, reported weak or non-meaningful relationships between C-class flare forcing and differential TEC under the tested estimation methods. That study also showed that the method used to define the background and perturbation matters. Accordingly, the current result is best described as a weak association between flare magnitude and the absolute TEC values in this dataset, not as evidence that C-class flares produce no ionospheric response.

4.2 Solar-activity Indices and Illumination Geometry

The magnitude-F10.7 coefficient (r = 0.331) is the largest positive magnitude association in the matrix. F10.7 is a broad solar-activity proxy rather than an instantaneous flare irradiance measurement, so the coefficient should be understood as contextual co-variation within the study interval. Similarly, SSN is a background activity index and not an event-scale measure of flare energy. The repeated use of daily index values across multiple same-day flares further limits the independence of the event-level coefficient.

The positive magnitude-SZA coefficient (r = 0.227) should not be interpreted as evidence that terrestrial observing geometry affects whether GOES detects a flare. Instead, SZA is relevant to the ionospheric response at a terrestrial location because atmospheric illumination and path length vary with solar zenith angle. Statistical flare studies have demonstrated substantial SZA dependence, particularly for stronger events (Le *et al.*, 2013), while global TEC analyses have additionally identified latitude and seasonal asymmetry in flare-associated TEC enhancements after accounting for SZA (Tsugawa *et al.*, 2006). Solar-disc position and the EUV spectrum can also be more informative for TEC enhancement than soft X-ray class alone (Zhang *et al.*, 2011). Case studies of recurrent X-class flare activity similarly report weak or inconsistent geoeffective responses despite high flare magnitude, underscoring that flare class alone is a limited predictor of ionospheric impact (Meena, 2026a). Because the terrestrial location and timestamp convention used for SZA are not preserved in the retained compilation, the present SZA coefficient is reported only as descriptive covariance and no site-specific geometric mechanism is assigned.

4.3 Plasma-temperature Associations

The mean Te exceeded the mean Ti, and Ti and Te were moderately positively associated (r = 0.372). Such ordering is physically plausible in portions of the ionosphere, but plasma temperature depends strongly on altitude, local time, latitude, season, solar activity, and energy balance. Empirical modelling and satellite observations demonstrate substantial spatial and solar-activity dependence of both Te and Ti (Köhnlein, 1986; Truhlik *et al.*, 2009). Consequently, the mean Ti/Te ratio of approximately 0.70 is reported as a descriptive property of the compiled dataset rather than as a universal or site-specific ionospheric state.

The negative association between Te and SZA (r = -0.573) is the largest absolute-magnitude off-diagonal coefficient involving Te. Without the altitude and geographic context of the temperature values, however, this pattern cannot be assigned a unique physical mechanism. The weaker negative magnitude-Te coefficient (r = -0.185) is likewise insufficient to support a collisional-cooling explanation or any other flare-specific mechanism. Such mechanistic statements would require measurement provenance and control for local time, density, altitude, and background conditions.

4.4 Background Variability and Study Limitations

TEC variability on daily to longer timescales reflects both solar and geomagnetic forcing. Multi-parameter studies have shown that TEC can covary with solar UV/X-ray flux, F10.7, geomagnetic indices, and other space-weather variables, often with non-zero time lags (Feng *et al*., 2023; Morozova *et al*., 2020; Gour *et al*., 2024). The present dataset does not include a documented event-level geomagnetic control series in the analysis, so the observed TEC variance cannot be partitioned among flare irradiation, background solar activity, geomagnetic forcing, and intrinsic ionospheric dynamics.

Six limitations define the scope of the conclusions. First, product-level provenance for TEC, Ti, and Te and the location/timing convention for SZA are incomplete in the retained event table. Second, absolute TEC was analysed rather than a pre-flare/post-flare perturbation metric. Third, daily solar indices may be repeated across multiple events, producing flare-record-weighted correlations and reducing the effective independent information; no cluster-adjusted sensitivity analysis is presented. Fourth, geomagnetic activity and site-specific local-time/latitude effects were not explicitly controlled. Fifth, the retained metadata do not establish whether the two calendar dates absent from the 75 represented days were zero-event days or missing/unretained source records. Sixth, the supplied study materials do not include a public repository accession for the 624-row event table or analysis code. These limitations do not alter the arithmetic of the reported descriptive summaries, but they constrain reproducibility and preclude causal statements about immediate flare-induced TEC or temperature changes.

A definitive event-response analysis would require traceable high-cadence GNSS TEC or ionospheric measurements with station coordinates, local time, SZA, altitude where relevant, flare start/peak/end times, pre-flare baselines, quiet-control periods, and concurrent geomagnetic indices. Differential TEC or TEC-rate metrics could then be modelled against GOES soft X-ray and EUV forcing while accounting for repeated events within days and spatially varying illumination.

5. Conclusions

1. The compiled dataset contains 624 C-class flare records between 1 January and 18 March 2025. The mean magnitude was C3.87 and the mean duration was 19.9 min. The retained source compilation contains 75 represented days within the 77-calendar-day interval, equivalent to 8.32 events per represented day and 8.10 events per calendar day; the status of the two unrepresented dates cannot be resolved from retained metadata.
2. Flare magnitude showed a weak-to-moderate descriptive association with F10.7 (r = 0.331) and weaker associations with SZA (r = 0.227) and SSN (r = 0.146). These values describe co-variation within the retained dataset and are neither event-independent inferential estimates nor evidence of direct physical forcing among the paired variables.
3. The flare-magnitude association with absolute TEC was negligible (r = 0.032). Because the study does not use event-centred ΔTEC, this result does not establish the absence of a C-class flare effect on the ionosphere.
4. Mean Ti and Te were 1168 K and 1694 K, respectively, with a mean Ti/Te ratio near 0.70. The temperature statistics are descriptive because altitude, site, and product-level provenance are incomplete in the compiled dataset.
5. The results support a conservative interpretation: frequent C-class flares in this interval were embedded in background solar and ionospheric variability that is not captured by flare class alone. The present coefficients should therefore be regarded as descriptive properties of the retained compilation. Event-response studies should use traceable high-cadence, event-centred measurements, explicit geomagnetic and illumination controls, day-cluster-aware statistical methods, and recoverable data-product provenance.

Data Availability

The analysis is based on an author-compiled event table derived from public space-weather records. The supplied study materials do not include a public repository accession for the complete 624-row event table or analysis code, and variable-level station, altitude, product/version, retrieval, and geographic metadata for some ionospheric variables are not retained. The manuscript therefore does not claim that the exact TEC, Ti, Te, or SZA series can be independently reconstructed from the generic source-agency names alone. The reported numerical results should be interpreted as a descriptive analysis of the retained compilation; exact independent reconstruction would require recovery of the missing provenance together with release of the event table, data dictionary, and analysis workflow.

Acknowledgements

The author did not receive any specific grant from funding agencies in the public, commercial, or not-for-profit sectors for this research.

Declaration of AI Use

This manuscript was prepared through the intellectual contributions of the author(s) to the study design, data analysis, interpretation of results, and scholarly content. Grammarly and ChatGPT were used solely to assist with grammatical refinement and reference formatting during manuscript revision. The author(s) accept full responsibility for the accuracy, integrity, and final content of the manuscript.

Competing Interests

Author has declared that no competing interests exist.

References

Bakdash, J. Z., & Marusich, L. R. (2017). Repeated measures correlation. *Frontiers in Psychology, 8*, Article 456. https://doi.org/10.3389/fpsyg.2017.00456

Feng, J., Zhang, Y., Li, W., Han, B., Zhao, Z., Zhang, T., & Huang, R. (2023). Analysis of ionospheric TEC response to solar and geomagnetic activities at different solar activity stages. *Advances in Space Research, 71*(5), 2225–2239. https://doi.org/10.1016/j.asr.2022.10.032

Gopalswamy, N., Xie, H., Yashiro, S., Akiyama, S., Mäkelä, P., & Usoskin, I. G. (2012). Properties of ground level enhancement events and the associated solar eruptions during Solar Cycle 23. *Space Science Reviews, 171*(1–4), 23–60. https://doi.org/10.1007/s11214-012-9890-4

Gour, P. S., Meena, A. K., Verma, P. L., Soni, S., Sharma, J., & Yadav, V. (2024). Correlation analysis of key parameters associated with solar activity and geomagnetic disturbances throughout 2023. *European Academic Research, 11*(12), 1494–1504. https://doi.org/10.5281/zenodo.21277354

Köhnlein, W. (1986). A model of the electron and ion temperatures in the ionosphere. *Planetary and Space Science, 34*(7), 609–630. https://doi.org/10.1016/0032-0633(86)90039-5

Le, H., Liu, L., Chen, Y., & Wan, W. (2013). Statistical analysis of ionospheric responses to solar flares in solar cycle 23. *Journal of Geophysical Research: Space Physics, 118*(1), 576–582. https://doi.org/10.1029/2012JA017934

Liu, J. Y., Lin, C. H., Chen, Y. I., Lin, Y. C., Fang, T. W., Chen, C. H., Chen, Y. C., & Hwang, J. J. (2006). Solar flare signatures of the ionospheric GPS total electron content. *Journal of Geophysical Research: Space Physics, 111*, Article A05308. https://doi.org/10.1029/2005JA011306

Meena, A. K. (2026a). Recurrent X-class flare activity from NOAA Active Region 4366 and its weak geoeffective response: A case study of the solar-terrestrial event (1–6 February 2026). *International Astronomy and Astrophysics Research Journal, 8*(1), 94–101. https://doi.org/10.9734/iaarj/2026/v8i1127

Meena, A. K., & Gour, P. S. (2024). Investigating Asia's low-latitude ionosphere's pulse during the spectacular September 2017 solar storms. *Tuijin Jishu/Journal of Propulsion Technology, 45*(1), 3322–3334. https://doi.org/10.5281/zenodo.21276970

Meena, A. K., Gour, P. S., & Soni, S. (2024). The effects of strong and weak solar flares on the total electron content in the ionospheric ionosphere during the 2011 solar peak. *African Journal of Biomedical Research, 27*(4S), 2422–2433. https://doi.org/10.53555/AJBR.v27i4S.2421

Meena, M. K., Meena, A. K., & Gour, P. S. (2022). Analysis of coronal mass ejections and solar flares. *International Journal of Innovative Research & Growth, 11*, 70–73. https://doi.org/10.26671/IJIRG.2022.3.11.104

Morozova, A. L., Barlyaeva, T. V., & Barata, T. (2020). Variations of TEC over Iberian Peninsula in 2015 due to geomagnetic storms and solar flares. *Space Weather, 18*(11), e2020SW002516. https://doi.org/10.1029/2020SW002516

Saharan, S., Maurya, A. K., Dube, A., Patil, O. M., Singh, R., & Sharma, H. (2023). Low latitude ionospheric TEC response to the solar flares during the peak of solar cycle 24. *Advances in Space Research, 72*(9), 3890–3902. https://doi.org/10.1016/j.asr.2023.07.015

Truhlik, V., Triskova, L., Bilitza, D., & Podolska, K. (2009). Variations of daytime and nighttime electron temperature and heat flux in the upper ionosphere, topside ionosphere and lower plasmasphere for low and high solar activity. *Journal of Atmospheric and Solar-Terrestrial Physics, 71*(17–18), 2055–2063. https://doi.org/10.1016/j.jastp.2009.09.013

Tsugawa, T., Sadakane, T., Sato, J., Otsuka, Y., Ogawa, T., Shiokawa, K., & Saito, A. (2006). Summer–winter hemispheric asymmetry of sudden increase in ionospheric total electron content induced by solar flares: A role of O/N_2 ratio. *Journal of Geophysical Research: Space Physics, 111*, Article A11316. https://doi.org/10.1029/2006JA011951

Vaswani, L. K., Gour, P. S., Meena, A. K., & Soni, S. (2022). Geomagnetic storm in association with solar activities. *International Journal of Innovative Research & Growth, 11*, 143–148. https://doi.org/10.26671/IJIRG.2022.4.11.103

Zhang, D. H., Mo, X. H., Cai, L., Zhang, W., Feng, M., Hao, Y. Q., & Xiao, Z. (2011). Impact factor for the ionospheric total electron content response to solar flare irradiation. *Journal of Geophysical Research: Space Physics, 116*, Article A04311. https://doi.org/10.1029/2010JA016089

Zhang, S.-R., Coster, A. J., Erickson, P. J., Goncharenko, L. P., Rideout, W., & Vierinen, J. (2019). Traveling ionospheric disturbances and ionospheric perturbations associated with solar flares in September 2017. *Journal of Geophysical Research: Space Physics, 124*(7), 5894–5917. https://doi.org/10.1029/2019JA026585

Peer-review history:
The peer review history for this paper can be accessed here:
https://pr.sdiarticle5.com/review-history/166147